

Preparation, Crystal Structures, and Magnetic and ESR Properties of Molecular Assemblies of Ferrocenium Derivatives and Paramagnetic Polyoxometalates

Stéphane Golhen,[†] Lahcène Ouahab,^{*,†} Daniel Grandjean,[†] and Philippe Molinié[‡]

Laboratoire de Chimie du Solide et Inorganique Moléculaire UMR 6511, Groupe Matériaux Moléculaires, Université de Rennes I, Av. Général Leclerc, 35042 Rennes Cedex, France, and Institut des Matériaux Nantes, 2 rue de la Houssinière, 44072 Nantes Cedex, France

Received September 25, 1997

The synthesis, X-ray crystal structures, and ESR and magnetic properties of the anhydrous salt $\text{Na}_3[\text{Cr}(\text{OH})_6\text{Mo}_6\text{O}_{18}] \cdot 6(\text{CH}_3)_2\text{SO}$ (**CrDMSO**) containing the Anderson–Evans polyanion, of two new molecular compounds based on this polyanion ($[\text{Fe}(\text{C}_5\text{Me}_5)_2]_3[\text{Cr}(\text{OH})_6\text{Mo}_6\text{O}_{18}] \cdot 20\text{H}_2\text{O}$ [**FeCr(1)**], $\text{Na}[\text{Fe}(\text{C}_5\text{Me}_5)_2]_2[\text{Cr}(\text{OH})_6\text{Mo}_6\text{O}_{18}] \cdot 3\text{H}_2\text{O}$ [**FeCr(2)**]), and of another based on a Keggin polyanion, $[\text{Fe}(\text{C}_5\text{Me}_5)_2]_4[\text{HPCu}(\text{H}_2\text{O})\text{W}_{11}\text{O}_{39}] \cdot 6\text{CH}_3\text{CN}$ (**FeCu**), are reported. **CrDMSO**: monoclinic, $C2/c$, $a = 25.37(2)$ Å, $b = 14.632(2)$ Å, $c = 15.455(6)$ Å, $\beta = 123.17(4)^\circ$, $Z = 4$. **FeCr(1)**: triclinic, $P\bar{1}$, $a = 12.489(3)$ Å, $b = 14.113(3)$ Å, $c = 15.662(4)$ Å, $\alpha = 101.55(2)^\circ$, $\beta = 105.82(2)^\circ$, $\gamma = 110.23(2)^\circ$, $Z = 1$. **FeCr(2)**: monoclinic, $P2_1/n$, $a = 10.015(2)$ Å, $b = 7.722(6)$ Å, $c = 25.137(5)$ Å, $\beta = 90.626(9)^\circ$, $Z = 2$. **FeCu**: monoclinic, $P2_1/n$, $a = 15.596(7)$ Å, $b = 15.138(3)$ Å, $c = 25.921(12)$ Å, $\beta = 97.53(2)^\circ$, $Z = 2$. In the compound **FeCr(1)** the $\text{Fe}(\text{C}_5\text{Me}_5)_2$ units are perpendicular to each other and form a centrosymmetrical group of three cations, which alternates with the planar $[\text{Cr}(\text{OH})_6\text{Mo}_6\text{O}_{18}]^{3-}$ anion to form perpendicular mixed chains along the $[21\bar{1}]$ and $[2\bar{1}1]$ directions. In the compound **FeCu**, the decamethylferrocenium units form a polyhedral structure which encapsulates the Keggin polyanion. The magnetic properties indicate that the salts containing metallocenium radicals present weak antiferromagnetic interactions obeying the Curie–Weiss expression $\chi = C/(T - \Theta)$ with small negative values for Θ (**FeCr(1)**, $\Theta = -0.5$, -0.4 ; **FeCr(2)**, $\Theta = -0.6$; **FeCu**, $\Theta = -0.8$). The ESR spectra for compounds containing chromium atoms may reveal a zero field splitting of the central chromium atom of the Anderson–Evans polyanions, which is directly related to the local symmetry of the chromium in its octahedral site.

Introduction

Polyoxometalates (POM) are of great interest because of the richness of their structural and electronic properties.^{1–3} These inorganic anions are investigated in many fields of research such as catalysis, biology, medicine, and materials science.^{4,5} For the particular class of molecular materials, the potentialities of these molecular metal oxides are exemplified by the well-known Keggin structure $[\text{XM}_{12}\text{O}_{40}]^{n-}$ in the following points: (i) This polyanion is a strong electron acceptor. (ii) It can be diamagnetic or paramagnetic depending on the nature and the oxidation state of the central heteroatom X and the outer transition metal M. (iii) It has been demonstrated also that one or more terminal oxygen atoms can be substituted by organic ligands.^{4,5} In previous works, we have used the polyoxometalates as components in charge-transfer salts,^{6–11} in materials associating mobile and localized magnetic electrons,^{12,13} and more recently

in compounds containing the organometallic decamethylferrocenium cation $\text{Fe}(\text{C}_5\text{Me}_5)_2^+$.¹⁴ These salts were formulated as $[\text{Fe}(\text{C}_5\text{Me}_5)_2]_4(\text{POM})(\text{solv})_n$, where $\text{POM} = [\text{SiMo}^{\text{VI}}_{12}\text{O}_{40}]^{4-}$, $[\text{SiW}^{\text{VI}}_{12}\text{O}_{40}]^{4-}$, $[\text{PMo}^{\text{V}}\text{Mo}^{\text{VI}}_{11}\text{O}_{40}]^{4-}$, and $[\text{HFeW}_{12}\text{O}_{40}]^{4-}$ and $\text{solv} = \text{H}_2\text{O}$, $\text{C}_3\text{H}_7\text{ON}$ (DMF), and CH_3CN . The $\text{Fe}(\text{C}_5\text{Me}_5)_2$ units form either infinite 1-D chains or a 3-D sublattice without significant magnetic interactions. Continuing our efforts in this direction, and with the aim to enhance the magnetic interactions between the POM and the $(\text{Fe}(\text{C}_5\text{Me}_5)_2)^+$ units, we have investigated compounds containing substituted Keggin¹⁵ polyanions such as $[\text{XM}'\text{W}_{11}\text{O}_{40}]^{n-}$, where $\text{M}' = \text{Fe}^{\text{III}}$, Cu^{II} , Ni^{II} , Cr^{III} , Mn^{III} , and Co^{II} , and the planar Anderson–Evans¹⁶ anions $[\text{M}'(\text{OH})_6\text{Mo}_6\text{O}_{18}]^{3-}$, where $\text{M}' = \text{Cr}^{\text{III}}$ and Ni^{II} (see Chart 1).

[†] Université de Rennes I.

[‡] Institut des Matériaux Nantes.

(1) Souchay, P. *Ions Minéraux Condensés*; Masson: Paris, 1969.

(2) Pope, M. T. *Heteropoly and Isopoly Oxometalates*; Springer-Verlag: New York, 1983.

(3) Evans, H. T., Jr. *Perspect. Struct. Chem.* **1971**, *4*, 1.

(4) Pope, M. T.; Müller, A. *Angew. Chem., Int. Ed. Engl.* **1991**, *30*, 34 and references therein.

(5) Pope, M. T.; Müller, A., Eds. *Polyoxometalates: from Platonic Solids to Anti-retroviral activity*; Kluwer Acad. Pub.: Dordrecht, The Netherlands, 1994.

(6) Ouahab, L.; Bencharif, M.; Grandjean, D. *C. R. Acad. Sci. Paris, Ser.* **2** **1988**, 749.

(7) Triki, S.; Ouahab, L.; Padiou, J.; Grandjean, D. *J. Chem. Soc., Chem. Commun.* **1989**, 1068.

(8) Ouahab, L.; Triki, S.; Grandjean, D.; Bencharif, M.; Garrigou-Lagrange, C.; Delhaès, P. In *Lower-Dimensional Systems and Molecular Crystals*; Metzger, R. M., Day, P., Papavassillou, G. C., Eds.; Plenum Press: New York, 1991; pp B248, 185.

(9) Gómez-García, C. J.; Coronado, E.; Triki, S.; Ouahab, L.; Delhaès, P. *Adv. Mater.* **1993**, 283.

(10) Mhanni, A.; Ouahab, L.; Peña, O.; Grandjean, D.; Garrigou-Lagrange, C.; Delhaès, P. *Synth. Met.* **1991**, 1703.

(11) Ouahab, L. In ref 5.

(12) Ouahab, L.; Bencharif, M.; Mhanni, A.; Pelloquin, D.; Halet, J. F.; Peña, O.; Padiou, J.; Grandjean, D.; Garrigou-Lagrange, C.; Amiel, J.; Delhaès, P. *Chem. Mater.* **1992**, *4*, 666.

(13) Gómez-García, C. J.; Ouahab, L.; Gimenez-Saiz, C.; Triki, S.; Coronado, E.; Delhaès, P. *Angew. Chem., Int. Ed. Engl.* **1994**, *33*, 223.

(14) Le Maguères, P.; Ouahab, L.; Golhen, S.; Peña, O.; Gómez-García, C. J.; Delhaès, P. *Inorg. Chem.* **1994**, *33*, 5180.

(15) Keggin, J. F. *Proc. R. Soc. London, Ser. A* **1934**, 75.

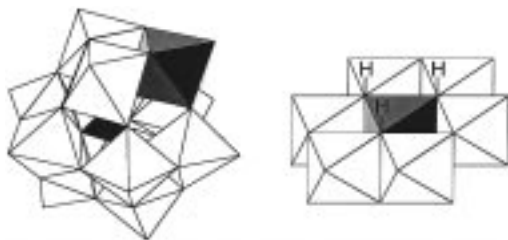
(16) Anderson, J. S. *Nature (London)* **1937**, 850.

Table 1. Crystallographic Data

	CrDMSO	FeCr(1)	FeCr(2)	FeCu
formula	CrMo ₆ Na ₃ O ₃₀ S ₆ C ₁₂ H ₄₂	CrMo ₆ Fe ₃ O ₄₄ C ₆₀ H ₁₃₆	CrMo ₆ Fe ₂ O ₂₇ C ₂₀ H ₃₂ Na	PW ₁₁ Fe ₄ CuO ₄₀ C ₉₂ H ₁₄₁ N ₆
space group	C2/c (No. 15)	P1̄ (No. 2)	P2 ₁ /n (No. 14)	P2 ₁ /n (No. 14)
a, Å	25.37(2)	12.489(3)	10.015(2)	15.596(7)
b, Å	14.632(2)	14.113(3)	7.722(6)	15.138(3)
c, Å	15.455(6)	15.662(4)	25.137(5)	25.921(12)
α, deg	90	101.55(2)	90	90
β, deg	123.17(4)	105.82(2)	90.626(9)	97.53(2)
γ, deg	90	110.23(2)	90	90
V, Å ³	4803(4)	2355.7(9)	1944(2)	6067(4)
Z	4	1	2	2
fw	1555.4	2356.9	1466.8	4311.4
d _{calc} , g·cm ⁻³	2.151	1.661	2.506	2.360
T, K	293	293	293	287
μ, mm ⁻¹	2.104	1.412	2.963	11.099
λ, Å	0.710 73	0.710 73	0.710 73	0.710 73
R indices				
R1 ^a	0.0253	0.0432	0.0648	0.0817
wR2 ^b	0.0891	0.0968	0.1592	0.1787

$$^a R1 = \sum ||F_o| - |F_c|| / \sum |F_o|. \quad ^b wR2 = \{ \sum [w(F_o^2 - F_c^2)^2] / \sum [w(F_o^2)^2] \}^{1/2}.$$

Chart 1. α-Keggin [XM'W₁₁O₄₀]ⁿ⁻ (M' = Fe^{III}, Cu^{II}, Ni^{II}, Cr^{III}, Mn^{III}, Co^{II}) and Anderson–Evans [M'(OH)₆Mo₆O₁₈]ⁿ⁻ (M' = Ni^{II}, Cr^{III}; M = Mo, W) Paramagnetic Polyanions, Where Gray Octahedra Contain the Paramagnetic M' Ion



In this later anion, the chromium atom is coordinated to six OH groups. Each oxygen atom of these groups bridges the chromium atom with two molybdenum atoms. The planar shape of this anion and the presence of the OH groups may favor the intermolecular interactions through hydrogen bonding. Besides, the central position of the paramagnetic transition metal could give rise to magnetic exchange. In this paper, we report the synthesis and the crystal structure of the unprecedented anhydrous salt Na₃[Cr(OH)₆Mo₆O₁₈·6(CH₃)₂SO] abbreviated **CrDMSO**, which consists of an Anderson–Evans polyanion where DMSO molecules substitute water molecules. We report also the synthesis, crystal structures, and magnetic and ESR characterizations of two decamethylferrocenium salts of the anion, [Fe^{III}(C₅Me₅)₂]₃[Cr(OH)₆Mo₆O₁₈·20H₂O] [**FeCr(1)**] and Na[Fe(C₅H₅)₂]₂[Cr(OH)₆Mo₆O₁₈·3H₂O] [**FeCr(2)**], and a decamethylferrocenium salt of a paramagnetic Keggin anion, [Fe(C₅Me₅)₂]₄[HPCu(H₂O)W₁₁O₃₉]·6CH₃CN (**FeCu**).

Experimental Section

Preparation of Compounds. Fe(C₅Me₅)₂,¹⁷ [Fe(C₅Me₅)₂]BF₄,¹⁸ [(C₄H₉)₄N]₄[HPCu(H₂O)W₁₁O₃₉],¹⁹ and Na₃[Cr(OH)₆Mo₆O₁₈]·8H₂O²⁰ were prepared according to the literature. All necessary reagents and solvents were purchased from Aldrich.

Na₃[Cr(OH)₆Mo₆O₁₈]·6[(CH₃)₂SO] (CrDMSO). A vigorous stirring of Na₃[Cr(OH)₆Mo₆O₁₈]·8H₂O in DMSO at 25–30 °C during

several days yielded a pink solution. After removal of the insoluble materials, the resulting solution was allowed to stand in a draft at 25–30 °C for several weeks to yield pink crystals after evaporation. Despite the fact that DMSO is a very hygroscopic solvent, the compound is completely anhydrous as confirmed by the X-ray structure (see below).

[Fe(C₅Me₅)₂]₃[Cr(OH)₆Mo₆O₁₈]·20H₂O [FeCr(1)]. An aqueous solution of [Fe(C₅Me₅)₂]BF₄ (1 mmol in 20 mL) was mixed with a concentrated aqueous solution of 0.33 mmol of Na₃[Cr(OH)₆Mo₆O₁₈]·8H₂O (**NaCr**). The resulting green precipitate was filtered off and recrystallized in a small amount of 1/5 H₂O/CH₃CN mixture to give well-shaped green crystals. The filtrate, allowed to remain for several days, yielded smaller green crystals. The crystallographic cells of both crystals showed that these two methods of crystallization give the same compound. When the crystals are in contact with air, they lose their crystallinity and decompose quickly. The presence of 20 water molecules per formula unit was checked unambiguously by X-ray diffraction.

Na[Fe(C₅H₅)₂][Cr(OH)₆Mo₆O₁₈]·3H₂O [FeCr(2)]. Crystal growth was performed in a glass H-cell where the two compartments are separated by a fine porosity glass frit. An aqueous concentrated solution of 1 mmol of [Fe(C₅H₅)₂]BF₄ is added to one compartment, and a concentrated solution of 0.33 mmol of **NaCr** in water is added to the other one. Well-shaped octahedral dark green crystals which appear after 2 days are allowed to grow for 2 weeks.

[Fe(C₅Me₅)₂]₄[HPCu(H₂O)W₁₁O₃₉]·6CH₃CN (FeCu). The mixture of an acetonitrile solution of (Bu₄N)₄[HPCu(H₂O)W₁₁O₄₀] (**Cu**) (0.25 mmol in 20 mL) and an acetonitrile solution of [Fe(C₅Me₅)₂]BF₄ (1.0 mmol in 10 mL) gave a limpid solution which is concentrated by slow evaporation. The blue green crystals are preserved in their mother liquor. When the crystals are in contact with air, they lose their crystallinity and decompose quickly after the escape of the acetonitrile molecules from the lattice.

Crystallographic Data Collection and Structure Determination. Single crystals were mounted on an Enraf-Nonius CAD4 diffractometer equipped with a graphite-monochromated Mo Kα radiation source (λ = 0.710 73 Å). The air-unstable crystals were sealed in a Lindemann glass capillary with their mother liquor, and the data were collected at 287 K for compound **FeCu** and 293 K for the others. Cell dimensions and an orientation matrix for data collection were obtained from least-squares refinement, using the setting angles of 25 centered reflections. The crystal data are summarized in Table 1. The intensities were collected by θ–2θ scans. No significant decay was revealed on the three standard reflections measured every 1 h during data collection, except for **FeCu** for which a decay correction was applied. Although it was sealed in a Lindemann glass capillary, it continued to degrade during the data collection. Lorenz polarization and semiempirical absorption corrections (ψ-scan method)²¹ were applied to intensities for all data except **FeCr(2)** for which a DIFABS²² procedure was applied. Scattering factors and corrections for anomalous dispersion

(17) King, R. B.; Bisnette, M. B. *J. Organomet. Chem.* **1967**, *8*, 287.

(18) Hendrickson, D. N.; Sohn, Y. S.; Gray, H. B. *Inorg. Chem.* **1971**, *10*, 1559.

(19) Galan-Mascaros, J. R.; Giménez-Saiz, C.; Triki, S.; Gómez-García, C. J.; Coronado, E.; Ouahab, L. *Angew. Chem., Int. Ed. Engl.* **1995**, *34*, 1460.

(20) Perloff, A. *Inorg. Chem.* **1970**, *9*, 2228.

were taken from ref 23. All structures were solved with SHELXS-86²⁴ and refined with SHELXL-93²⁵ programs by full-matrix least-squares methods, on F^2 . The positional disorders between the sodium atom and the water molecule in **FeCr(2)** and between tungsten atoms and copper atom in **FeCu** were solved by refinement of the occupancy factor of the heavy atoms. Additionally for this compound, high thermal motion and/or disorder was also observed for methyl groups of the $\text{Fe}(\text{C}_5\text{Me}_5)_2^+$ units. Due to this disorder the refinements were applied to the positional and anisotropic thermal parameters for heavy atoms. Only thermal isotropic parameters were refined for others atoms and were fixed to $U = 0.10 \text{ \AA}^2$ for three of the methyl carbons and the solvent molecules.

Atomic coordinates and U_{eq} values for all compounds and the complete crystal structure results are given as Supporting Information.

Magnetic and ESR Spectroscopy Measurements. All magnetic studies were carried out on powder samples enclosed in a medical capsule. Magnetic susceptibility measurements were performed at 0.5 T after zero field cooling, in the temperature range 2–300 K with a SQUID magnetometer "MPMS-5" from Quantum Design Corp. Magnetization measurements were made at 2 and 5 K in the magnetic field range 0–5 T. The X-band ESR spectra were performed on a Bruker ER 200D-SRC spectrometer in the temperature range 100–300 K.

Results and Discussion

X-ray Crystal Structures. $\text{Na}_3[\text{Cr}(\text{OH})_6\text{Mo}_6\text{O}_{18}] \cdot 6[(\text{CH}_3)_2\text{SO}]$ (**CrDMSO**). The anion adopts the so-called Anderson–Evans structure. It consists of six $[\text{MoO}_6]$ octahedra surrounding the paramagnetic Cr^{III} ion, giving rise to a disklike structure.²⁰ The intramolecular bond length and bond angles are in the range of those reported for the hydrated salt $\text{Na}_3[\text{Cr}(\text{OH})_6\text{Mo}_6\text{O}_{18}] \cdot 8\text{H}_2\text{O}$.²⁰ A view of the anion projected onto the Cr–Mo fitted plane is shown in Figure 1a. A polyhedral representation of the structure viewed along the b axis is shown in Figure 1b. Six DMSO molecules are surrounding the polyanion. Three molecules are above the mean plane of the anion, and the three remaining molecules are below this plane. For all DMSO molecules, short distances (2.631 Å) are observed between their oxygen atoms and the oxygen atoms of the OH groups bonded to the central Cr atom of the polyanion (Figure 1b). These distances seem to indicate the presence of hydrogen bonding between the two units. Both Na1 and Na2 sodium atoms are coordinated to similar distorted octahedral surrounding (Figure 1b). The sodium ions are coordinated to oxygen atoms of both solvent (DMSO) and polyanions, each octahedron including four atoms of two neighboring anions and two from two different DMSO molecules. This situation is different from that observed in $\text{Na}_3[\text{Cr}(\text{OH})_6\text{Mo}_6\text{O}_{18}] \cdot 8\text{H}_2\text{O}$, where each octahedron includes four oxygen atoms from the same anion and two from water molecules of the solvent.²⁰

$[\text{Fe}(\text{C}_5\text{Me}_5)_2]_3[\text{Cr}(\text{OH})_6\text{Mo}_6\text{O}_{18}] \cdot 20\text{H}_2\text{O}$ [**FeCr(1)**]. The asymmetric unit contains one anion centered at the origin of the unit cell, one independent $\text{Fe}(\text{C}_5\text{Me}_5)_2^+$ cation, noted A (Fe2), in a general position and another one, noted B (Fe1), centered at the $(0, \frac{1}{2}, \frac{1}{2})$ center of symmetry, and 10 water molecules. In this crystal, 10 H_2O solvent molecules are arranged above and 10 others below the polyanion disk. The minimal O–O_w distances compare very well with the contacts observed in the hydrated salt²⁰ and which are attributed to

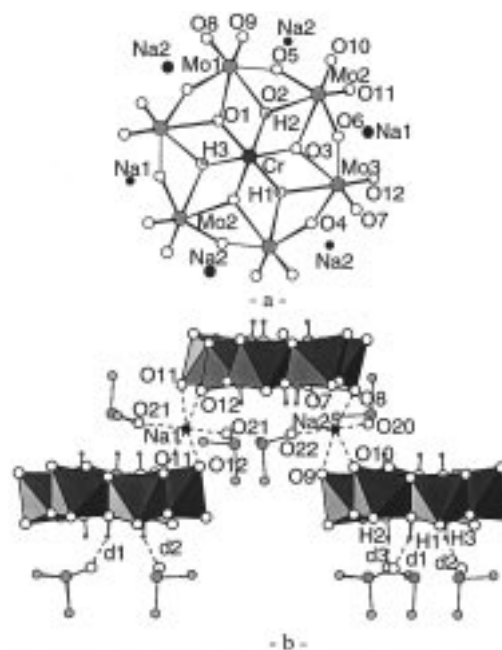


Figure 1. (a) View of the anion projected onto the Cr–Mo fitted plane. The atom names are similar in the three compounds containing the Anderson–Evans polyanion. Selected bond distances are given in Table 4. (b) Polyhedral representation of the structure of **CrDMSO** viewed along the b axis. Selected bond distances (Å): $d1 = \text{O}22\text{--O}1 = 2.631(4)$, $d2 = \text{O}21\text{--O}3 = 2.633(4)$, $d3 = \text{O}20\text{--O}2 = 2.634(4)$. Selected bond distances for sodium coordination (Å): $\text{Na}1\text{--O}21 = 2.360(3)$, $\text{Na}1\text{--O}12 = 2.454(4)$, $\text{Na}1\text{--O}11 = 2.755(4)$; $\text{Na}2\text{--O}20 = 2.361(4)$, $\text{Na}2\text{--O}22 = 2.359(4)$, $\text{Na}2\text{--O}8 = 2.460(4)$, $\text{Na}2\text{--O}10 = 2.461(4)$, $\text{Na}2\text{--O}7 = 2.755(4)$, $\text{Na}2\text{--O}9 = 2.755(4)$.

hydrogen bonds. A and B form a group of three cations (ABA) centered on B with their five-membered rings nearly perpendicular (Figure 2a). The dihedral angle between the cyclopentadienyl rings of two adjacent $\text{Fe}(\text{C}_5\text{Me}_5)_2^+$ unit is ca. $92.0(4)^\circ$. This group forms with the $[\text{Cr}(\text{OH})_6\text{Mo}_6\text{O}_{18}]^{3-}$ unit a mixed stack in a ... (ABA)–trianion–(ABA)... sequence along the nearly orthogonal $[2\bar{1}1]$ and $[21\bar{1}]$ directions. The angle between the two directions is about $86.18(1)^\circ$ and the minimal distance between Fe(A) and Fe(B) is $7.889(2) \text{ \AA}$, while the shorter one between Cr and cation A is $8.888(2) \text{ \AA}$. This mixed stack generates layers parallel to the (011) plane (Figure 2b), and the crystal structure results from the packing of these layers along a direction perpendicular to the previous (011) plane. The mean separation between two adjacent layers is about 8.17 \AA .

$\text{Na}[\text{Fe}(\text{C}_5\text{H}_5)_2]_2[\text{Cr}(\text{OH})_6\text{Mo}_6\text{O}_{18}] \cdot 3\text{H}_2\text{O}$ [**FeCr(2)**]. The asymmetric unit is constituted from one $\text{Fe}(\text{C}_5\text{H}_5)_2^+$ unit in a general position and a $[\text{Cr}(\text{OH})_6\text{Mo}_6\text{O}_{18}]^{3-}$ fragment centered at the origin. Refinement of the occupancy factors of the sodium site gave a value of 0.728, which corresponds to one Na cation and one water molecule randomly distributed on the same position, a value which is in agreement with the one expected for the neutral electronic charge of the compound. The minimal distance between the iron atoms of the two closest $\text{Fe}(\text{C}_5\text{H}_5)_2^+$ units is $6.741(4) \text{ \AA}$, while the shorter one between Cr and Fe is about $7.598(3) \text{ \AA}$. The structure is shown in Figure 3.

$[\text{Fe}(\text{C}_5\text{Me}_5)_2]_4[\text{HPCu}(\text{H}_2\text{O})\text{W}_{11}\text{O}_{39}] \cdot 6\text{CH}_3\text{CN}$ (**FeCu**). The asymmetric unit is constituted from two $\text{Fe}(\text{C}_5\text{Me}_5)_2^+$ units in general positions and one $[\text{HPCu}(\text{H}_2\text{O})\text{W}_{11}\text{O}_{39}]^{4-}$ polyanion centered at the origin of the unit cell. The polyanion has the disordered α -Keggin structure.¹⁵ In fact, due to the centering, the polyanion is disordered and consists of 12 corner-sharing MO_5 square pyramids plus 8 inner half-oxygens of the PO_4 group. This kind of disorder, which has been reported for a

(21) North, A. C. T.; Philips, D. C.; Mathews, F. S. *Acta Crystallogr., Sect. A* **1968**, A24, 351.

(22) Walker, N.; Stuart, D. *Acta Crystallogr.* **1983**, A39, 158.

(23) *International Tables for X-ray Crystallography*; Kynoch Press: Birmingham, U.K., 1974; Vol. IV.

(24) Sheldrick, G. M. *Acta Crystallogr.* **1990**, A46, 467.

(25) Sheldrick, G. M. *SHELXL 93, Program for the Refinement of Crystal Structures*; University of Göttingen: Göttingen, Germany, 1993.

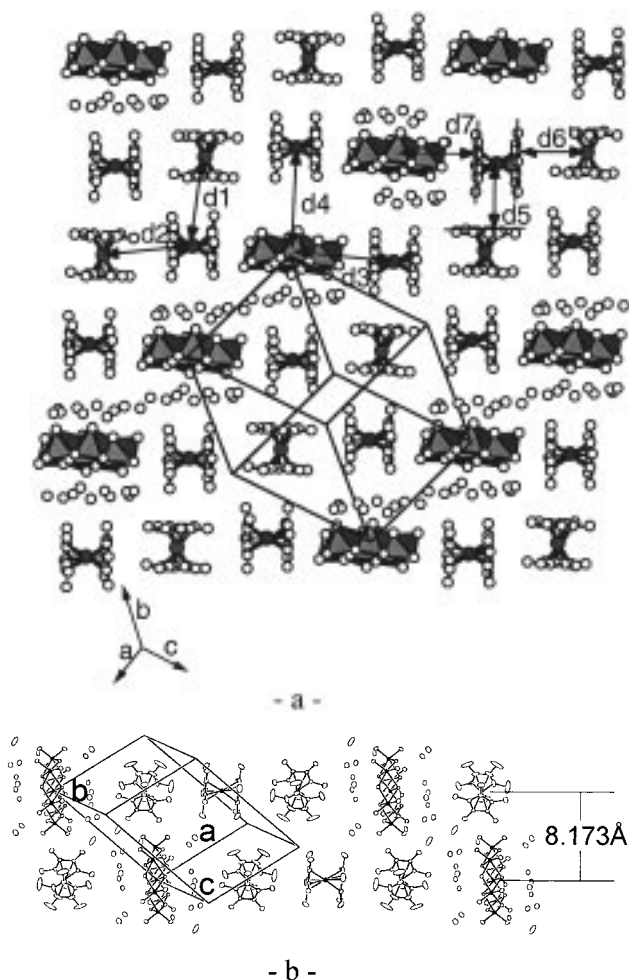


Figure 2. (a) Projection of the crystal structure of FeCr(1) onto the (011) plane with $d1 = 7.889$ Å, $d2 = 7.983$ Å, $d3 = 8.888$ Å, $d4 = 9.386$ Å, $d5 = 6.142$ Å, $d6 = 6.219$ Å, and $d7 = 7.139$ Å. (b) Packing of two adjacent layers along a direction perpendicular to the previous (011) plane.

number of salts containing large cations,^{12,26,27} was discussed in details by Evans and Pope.²⁸ Besides this orientational disorder, there is a positional disorder on the metallic sites. The refinements of the occupancy factors for the six independent metallic sites of the Keggin polyanion gave values of ca. 1 for three tungsten atoms (W1, W2, and W5), ca. 0.95 for two others (W3 and W4), and 0.80 for W6. This correspond to one copper atom for 11 tungsten atoms for overall anion. The instability of the crystals and the disorders observed account for the low accuracy of the structure. The structure is shown in Figure 4. In this structure, the $\text{Fe}(\text{C}_5\text{Me}_5)_2^+$ units are also orthogonal. The dihedral angle between the cyclopentadienyl rings of two adjacent Fe is ca. $99(2)^\circ$. Twelve $\text{Fe}(\text{C}_5\text{Me}_5)_2^+$ units form a polyhedron which contains in its cavity the $[\text{HPCu}(\text{H}_2\text{O})\text{W}_{11}\text{O}_{39}]^{4-}$ unit. The shortest Fe–Fe distance within the polyhedron is $7.705(8)$ Å, and the shortest Cu–Fe distance is $6.331(4)$ Å (Cu being distributed over the W3, W4, and W6 sites).

Thermogravimetric Analysis. Thermogravimetric analyses (TGA) of FeCr(1) were carried out under nitrogen flow. From

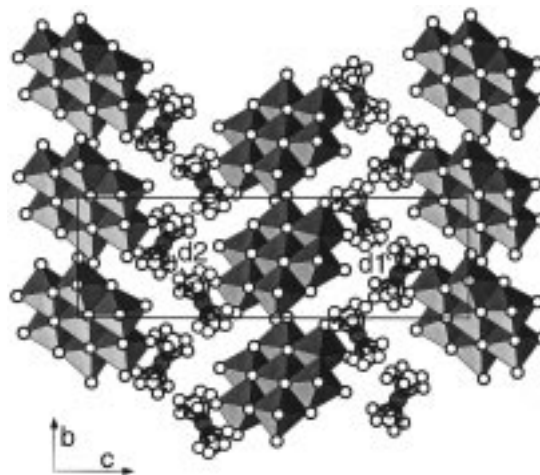


Figure 3. Projection of the crystal structure of FeCr(2) onto the (100) plane. $d1 = 6.741(4)$ Å, and $d2 = 6.938(5)$ Å.

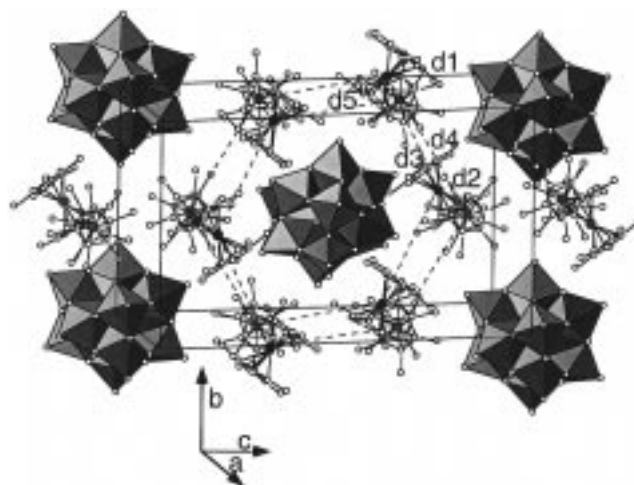


Figure 4. Unit cell of FeCu. Four polyanions and the methyl carbon atoms on the $\text{Fe}(\text{C}_5\text{Me}_5)_2$ units are omitted for clarity. $d1 = 7.705(8)$ Å, $d2 = 7.960(8)$ Å, $d3 = 8.361(5)$ Å, $d4 = 8.830(5)$ Å, and $d5 = 9.350(8)$ Å.

these analyses we observed that the 20 water molecules can be removed below 60°C . Above this temperature, the coordinated OH units are removed, and the compound decomposes. To estimate the influence of the water molecules on the magnetic properties, we prepared the dehydrated salt $[\text{Fe}(\text{C}_5\text{Me}_5)_2]_3[\text{Cr}(\text{OH})_6\text{Mo}_6\text{O}_{18}]$ (FeCrDH). This salt was obtained by heating FeCr(1) salt at 50°C under nitrogen.

Magnetic Properties. The molar susceptibility was corrected from the sample holder and diamagnetic contribution of all atoms by using Pascal's tables.²⁹ For all the compounds, the molar susceptibility measured under 0.5 T, in the temperature range 4.5–300 K, obeys a Curie–Weiss law $\chi = C/(T - \Theta)$ with weak negative values of the Weiss constant Θ . The constants resulting from susceptibility measurements are given in Table 2. The starting salts $\text{Na}_3[\text{Cr}(\text{OH})_6\text{Mo}_6\text{O}_{18}] \cdot 8\text{H}_2\text{O}$ and $(\text{Bu}_4\text{N})_4[\text{HPCu}(\text{H}_2\text{O})\text{W}_{11}\text{O}_{39}]$ abbreviated CrMo and Cu, respectively, are salts containing a unique magnetic center which

(26) Gómez-García, C. J.; Giménez-Saiz, C.; Triki, S.; Coronado, E.; Le Maguerès, P.; Ouahab, L.; Ducasse, L.; Sourisseau, C.; Delhaès, P. *Inorg. Chem.* **1995**, *34*, 4139.

(27) Attanazio, D.; Bonamico, M.; Fares, V.; Imperatori, P.; Suber, L. J. *Chem. Soc., Dalton Trans.* **1990**, 3221.

(28) Evans, H. T., Jr.; Pope, M. T. *Inorg. Chem.* **1984**, *23*, 501.

(29) The sample contribution M_{sh} was estimated from a Curie law variation $M_{\text{sh}} = (-0.38 \times 10^{-6} + 0.18 \times 10^{-6}/T)m$, m being the mass of the medical capsule (in g) and T being the temperature (in K). For diamagnetic contributions, see: (a) Selwood, P. W. *Magnetochemistry*; Interscience Publishers: New York, 1956. (b) Mabbs, F. E.; Machin, D. J. *Magnetism and Transition Metal Complexes*; Chapman and Hall Ltd.: London, 1973. (c) Kahn, O. *Molecular Magnetism*; VCH Publishers: New York, 1993.

Table 2. Magnetic Parameters Deduced from Magnetic Susceptibility Measurements at 0.5 T^a and from Magnetization Measurements Performed at 2 and 5 K under a Magnetic Field between 0 and 5 T^b

	FeCr(1)	FeCrDH	FeCr(2)	CrMo	FeCu	Cu
$C, ^a \text{ cm}^{-3} \cdot \text{K} \cdot \text{mol}^{-1}$	4.71/4.97	4.24	3.18	1.63	3.82/3.98	0.44
$\Theta, ^a \text{ K}$	-0.5/-0.4	-0.5	-0.6	-0.1	-0.8	-0.1
$C[(\text{FeCp}^*_2)]^a, \text{ cm}^{-3} \cdot \text{K} \cdot \text{mol}^{-1}$	1.03/1.11	0.87			0.84/0.88	
$C[(\text{FeCp})_2]^a, \text{ cm}^{-3} \cdot \text{K} \cdot \text{mol}^{-1}$			0.77			
g_{Briil}^b at 2 K	3.30	2.80	2.75	1.80	2.65	2.15
$C_a(\text{FeCp}^*_2)^b$ at 2 K, $\text{ cm}^{-3} \cdot \text{K} \cdot \text{mol}^{-1}$	1.03	0.73		1.53	0.66	0.43
$C_a(\text{FeCp}_2)^b$ at 2 K, $\text{ cm}^{-3} \cdot \text{K} \cdot \text{mol}^{-1}$			0.71			
g_{Briil}^b at 5 K	3.40	3.00			2.82	
$C_a(\text{FeCp}^*_2)^b$ at 5 K, $\text{ cm}^{-3} \cdot \text{K} \cdot \text{mol}^{-1}$	1.08	0.81			0.74	

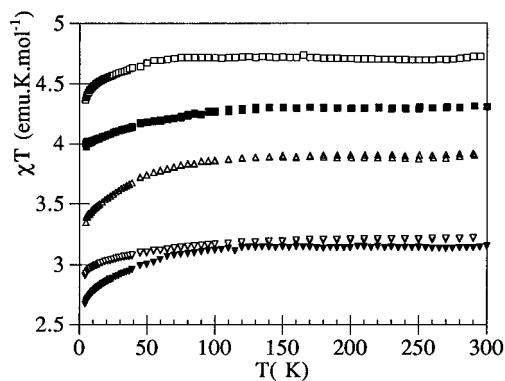
^a g_{Briil} was determined using the Brillouin expression ($M = N g \mu_B J B_J(x)$) with $x = g \mu_B J H_c / kT$ and we assumed $J = S$ for two independent systems: the $S = 3/2$, $g_{\text{Briil}} = 1.80$ (Cr^{3+}) or the $S = 1/2$, $g_{\text{Briil}} = 2.15$ (Cu^{2+}) from the polyanion, and the appropriate number of Cr^{3+} and Cu^{2+} ions are obtained from magnetization measurements performed on the starting materials [**CrMo**] and [**Cu**]. ^b C_a were calculated by the expression $C_a = [N(g_{\text{Briil}})^2 \mu_B^2 S(S+1)]/3k$.

allows one to calculate the Curie constant value of both the $\text{Fe}(\text{C}_5\text{Me}_5)_2^+$ and $\text{Fe}(\text{C}_5\text{H}_5)_2^+$ units in the case where the salts contain several magnetic centers.

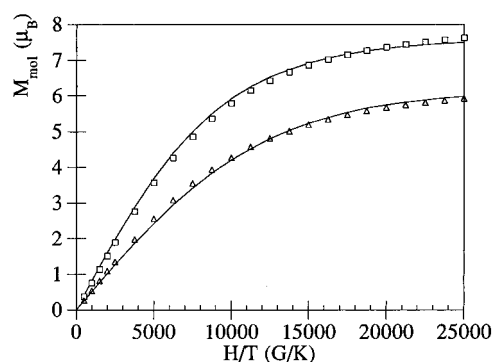
The small negative values of Θ are similar to those found in other ferrocenium or decamethylferrocenium complexes^{14,30–36} and suggest the absence of significant exchange interactions between organometallic fragments or inorganic polyanion and organometallic radicals.

The variation of χT versus T for all the compounds are plotted in Figure 5a. We observe for all the ferrocenium salts a decrease of χT with temperature below 60 K. This decrease is about 10% of the value at 300 K. These phenomena are almost of the same magnitude as those described previously¹⁴ and cannot be fully explained by a magnetic anisotropy of the g -factor or by a zero-field splitting of the paramagnetic ions Cu^{2+} , Cr^{3+} , or $\text{Fe}(\text{C}_5\text{Me}_5)_2^+$.^{29c} Moreover the experimental Curie constant values for $\text{Ca}(\text{FeCp}^*_2)$ and $\text{Ca}(\text{FeCp}_2)$ obtained at 2 K by magnetization measurements (Figure 5b) are, in all cases, lower than those calculated from the Curie constant for $\text{C}(\text{FeCp}^*_2)$ or $\text{C}(\text{FeCp}_2)$ (see Table 2). This fact may be indicative of weak intermolecular antiferromagnetic interactions at low temperature^{37–39} despite the long distances between magnetic centers. For the **FeCrDH** compound, the molar susceptibility is similar to that of **FeCr(2)** and leads to an average Curie constant of 4.24 for a molecular weight of 1996.9 $\text{g} \cdot \text{mol}^{-1}$, which is in agreement with the experiment. The averaged experimental Curie constant value for all $\text{Fe}(\text{C}_5\text{Me}_5)_2^+$ cations is around 0.92, which leads to a μ_{eff} (μ_{eff} is defined as $\mu_{\text{eff}} = (8C)^{1/2}$) close to $2.70 \mu_B$, a higher value than the one observed: $2.02–2.65 \mu_B$.¹⁴

ESR Spectra. Salts of ferrocenium and its derivatives are normally ESR silent at room temperature due to a short spin–lattice relaxation T_1 ;⁴⁰ at low temperature, they usually show a



- a -



- b -

Figure 5. (a) χT ($\text{emu} \cdot \text{K} \cdot \text{mol}^{-1}$) measured under 0.5 T versus T (K) plots for the **FeCr(1)** (\square), **FeCrDH** (\blacksquare), **FeCr(2)** (∇), and **FeCu** (\triangle) compounds. (b) Magnetization versus magnetic field at 2 K for compounds **FeCr(1)** (\square) and **FeCu** (\triangle). The solid line represents in each case the best fit to the Brillouin expression for two independent systems (Table 2).

very anisotropic axial signal with $g_{\parallel} \sim 3.8–4.4$ and $g_{\perp} \sim 1.2–1.9$.^{41–48} In contrast, the Cu^{II} and Cr^{III} ions give a detectable signal at room temperature. For an octahedral Cu^{II} ion ($3d^9$, 2D , $L = 2$, $S = 1/2$) with an axial distortion we have $g_{\parallel} \sim 2.15–$

- (30) Miller, J. S.; Calabrese, J. C.; Epstein, A. J.; Bigelow, W.; Zhang, J. H.; Reiff, W. M. *J. Chem. Soc., Chem. Commun.* **1986**, 1026.
 (31) Miller, J. S.; Calabrese, J. C.; Rommelmann, H.; Chittapeddi, S. R.; Zhang, J. H.; Reiff, W. M.; Epstein, A. J. *J. Am. Chem. Soc.* **1987**, 769.
 (32) Gebert, E.; Reis, A. H., Jr.; Miller, J. S.; Rommelmann, H.; Epstein, A. J. *J. Am. Chem. Soc.* **1982**, 104, 4403.
 (33) Candela, G. A.; Swartzendruber, L. J.; Miller, J. S.; Rice, M. J. *J. Am. Chem. Soc.* **1979**, 101, 2755.
 (34) Morrison, W. H., Jr.; Krogsrud, S.; Hendrickson, D. N. *Inorg. Chem.* **1973**, 12, 1998.
 (35) Wassermann, K.; Palm, R.; Lunk, H. J.; Fuch, J.; Steinfeldt, N.; Stosser, R. *Inorg. Chem.* **1995**, 34, 5029.
 (36) Hendrickson, D. N.; Sohn, Y. S.; Gray, H. B. *Inorg. Chem.* **1971**, 10, 1559.
 (37) Morrison, W. H., Jr.; Hendrickson, D. N. *Inorg. Chem.* **1975**, 14, 2331.
 (38) Cowan, D. O.; Candela, G. A.; Kaufman, F. *J. Am. Chem. Soc.* **1971**, 93, 3889.
 (39) Miller, J. S.; Epstein, A. J.; Reiff, W. M. *Chem. Rev.* **1988**, 201.

- (40) Fritz, H. P.; Keller, H. J.; Schwarzhans, K. E. *J. Organomet. Chem.* **1967**, 7, 105.
 (41) Duggan, M.; Hendrickson, D. N. *Inorg. Chem.* **1975**, 14, 955.
 (42) Morrison, W. H., Jr.; Hendrickson, D. N. *Inorg. Chem.* **1975**, 14, 2331.
 (43) Morrison, W. H., Jr.; Krogsrud, S.; Hendrickson, D. N. *Inorg. Chem.* **1973**, 12, 1998.
 (44) Prins, R.; Kortbeek, A. G. T. G. *J. Organomet. Chem.* **1971**, 33, C33.
 (45) Prins, R. *Mol. Phys.* **1970**, 19, 603.
 (46) Prins, R.; Reinders, F. J. *J. Am. Chem. Soc.* **1969**, 91, 4929.
 (47) Maki, A. H.; Berry, T. E. *J. Am. Chem. Soc.* **1965**, 87, 4437.
 (48) Goan, J. C.; Berg, E.; Podall, H. E. *J. Org. Chem.* **1964**, 29, 1975.

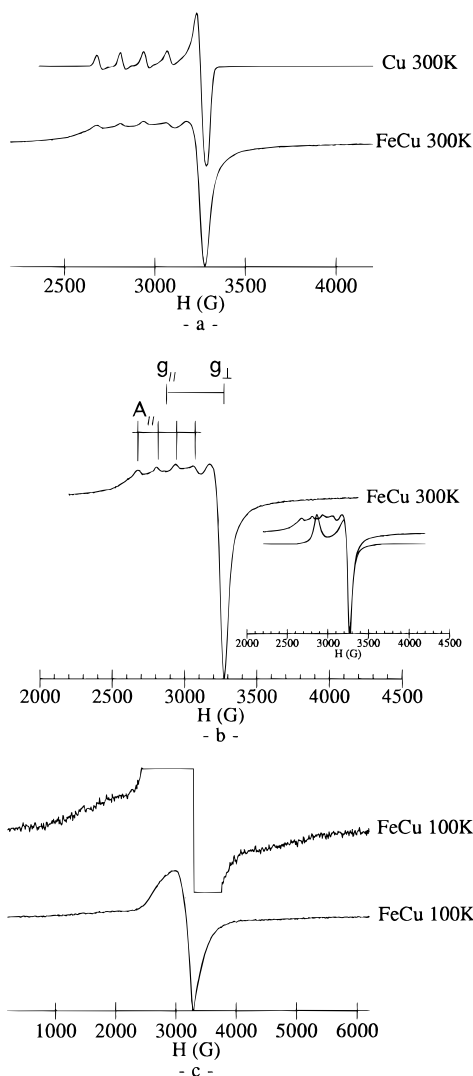


Figure 6. (a) ESR spectra of powder samples of the **FeCu** and **Cu** compounds at 9.416 GHz. (b) At 300 K, Cu^{II} contribution from the anionic part. Inset: Zeeman simulation for a powder sample of the Cu^{II} ion. (c) ESR spectra at 100 K of a powder sample of the **FeCu** compound. In the top part, the signal is magnified by 500 \times .

2.40 and $g_{\perp} \sim 2.0$ –2.10.^{49–52} For an octahedral Cr^{III} ($3d^3$, 4F , $L = 3$, $S = 3/2$) the situation may be more complex due to a possible zero-field splitting.⁵³

Copper-Containing Compounds. The ESR spectra (Figure 6a) of both **FeCu** and **Cu** compounds at 300 K show a rather similar feature. In fact, the magnetic measurement for these two salts indicates the presence of one electron in the Keggin polyanion (see Table 2) close to the expected value for a Cu^{II} ion ($S = 1/2$). This is in agreement with the ESR results, and their two spectra can be attributed to $S = 1/2$ octahedral Cu^{II} with an axial distortion and a hyperfine structure for the copper ($I = 3/2$) nucleus (from Figure 6b). We find the Zeeman parameters $g_{\parallel} \sim 2.350$, $g_{\perp} \sim 2.065$, $\Delta H_{\text{pp}} = 50$ G, and $A_{\parallel} = 128.7$ G and estimated $A_{\perp} = 61$ G. These values are in

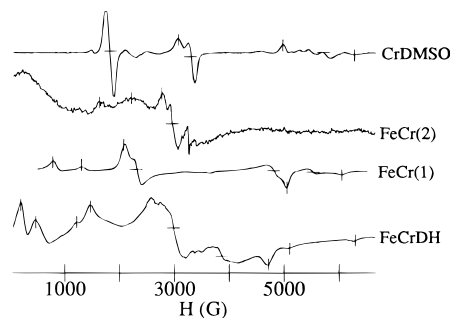


Figure 7. ESR spectra at 300 K of powder samples of the **FeCrDH**, **FeCr(1)**, **FeCr(2)**, and **CrDMSO** compounds at 9.416 GHz (\uparrow for vertice or shoulder and \downarrow for center; see Table 3).

Table 3. Selected g Values Deduced from the ESR Spectra for All of the Anderson–Evans Complexes^a

	Cr	CrDMSO	FeCr(1)	FeCr(1)	FeCr(2)	FeCrDH
T (K)	300	300	300	100	300	300
g			13.5 v	21.1 v		33.0 v
			6.6 v	10.1 v	10.2 i	14.4 v
						5.60 s
		3.72 i	3.75 v	4.16 v	4.04 v	4.60 v
	3.58 i		3.33 i	3.10 i	2.93 v	
					2.36 v	
		2.23 v			2.23 i	2.25 i
		2.05 i		2.02 v		
						1.75 i
	1.39 s	1.36 v	1.42 v	1.34 v		1.43 v
	1.18 i	1.24 i	1.29 i			1.32 v
		1.16 v	1.18 v	1.07 v		1.08 v
		0.72 i	0.86 v	0.83 v		0.95 v
						0.77?

^a i = center, v = vertice, and s = shoulder.

agreement with those found in the literature.⁴⁰ At 100 K (Figure 6c), the hyperfine structure is hidden by the increasing of the ΔH_{pp} (150 G). Besides we notice a very broad line under the Cu^{II} spectra with Zeeman parameters of $g_{\parallel} \sim 2.6$ and $g_{\perp} \sim 1.5$ and $\Delta H_{\text{pp}} = 1000$ G ($g_{\text{iso}} = 2.3$) or $g_{\text{iso}} = 2.1$ and $\Delta H_{\text{pp}} = 1800$ G which might arise from the $\text{Fe}(\text{C}_5\text{Me}_5)_2^+$ unit.

Chromium-Containing Compounds. The ESR spectra for compounds **CrDMSO**, **FeCr(1)**, **FeCr(2)**, and **FeCrDH** are given in Figure 7. The g values deduced from these spectra are given in Table 3. These spectra are rather complexes due to the zero-field splitting of the central chromium atom of the Anderson–Evans polyanions. This zero-field splitting is directly related to the local symmetry of the chromium in its octahedral environment.

As shown in Table 4, one can imagine two different deformations of the octahedron. The first one, called tetragonal, occurs along the C_4 axis ($\text{O}2-\text{Cr}-\text{O}2'$ in Table 4, I); the second one, called rhombic, takes place along the C_3 axis (Table 4, II). We report in Table 4 the geometrical parameters around the chromium atoms in our salts as well as those reported in both the $\text{Na}_3[\text{Cr}(\text{OH})_6\text{Mo}_6\text{O}_{18}] \cdot 8\text{H}_2\text{O}$ (**NaCr**) and $[\{\text{A}-\alpha\text{-SiO}_4\text{W}_9\text{O}_{30}(\text{OH})_3\text{Cr}_3\}_2(\text{OH})_3]^{11-}$ (**WCr6**)³⁵ salts in which rhombic and tetragonal deformations, respectively, have been observed. From the values given in Table 4, we observe homogeneous Cr–O and O–O distances for compounds **CrDMSO**, **FeCr(1)**, and **NaCr**. In particular, these geometrical parameters indicate a perfect octahedral environment of the Cr atom in **CrDMSO**, and accordingly, a well-defined ESR spectrum is observed for this compound (Figure 7). However, a tetragonal deformation, rather than a rhombic one, is observed for the **FeCr(2)** salt. The Cr–O2 distance (2.00 Å) is greater than the

(49) Ursu, I. *La résonance paramagnétique électronique*; Dunod: Paris, 1968.

(50) Abragam, A.; Bleaney, B. *La résonance paramagnétique électronique des ions de transition*; PUF: Paris, 1971.

(51) Wertz, A.; Bolton, R. *Electron spin resonance: elementary theory and practical applications*; McGraw-Hill: New York, 1972.

(52) Bencini, A.; Gatteschi, D. *Electron Paramagnetic Resonance of Exchange Coupled Systems*; Springer-Verlag: Berlin, Heidelberg, 1990.

(53) Pedersen, E.; Toftlund, H. *Inorg. Chem.* **1974**, *13*, 1603.

Table 4. Selected Bond Distances (Å) and Bond Angles (deg) for **CrDMSO**, **FeCr(1)**, **FeCr(2)**, **NaCr**, and the $[\{A-\alpha-SiO_4W_9O_{30}(OH)_3Cr_3\}_2(OH)_3]^{11-}$ Salt **WCr₆**³⁵

	CrDMSO ^a	FeCr(1) ^a	FeCr(2) ^a	NaCr ^b	WCr₆ ^c W6–W7
Distances					
Cr–O1	1.962(2)	1.971(4)	1.957(10)	1.986(3)	1.966–1.950
Cr–O1'					1.952–1.962
Cr–O2	1.959(2)	1.973(4)	1.996(8)	1.968(3)	2.044–2.029
Cr–O2'					1.970–1.955
Cr–O3	1.963(3)	1.969(4)	1.962(11)	1.972(2)	1.966–1.931
Cr–O3'					1.952–1.971
Mo1–O1	2.293(2)	2.281(4)	2.295(10)	2.347(3)	
Mo1–O2	2.282(2)	2.302(4)	2.272(10)	2.289(3)	
Mo2–O2	2.296(3)	2.305(4)	2.238(11)	2.294(2)	
Mo2–O3	2.278(2)	2.297(4)	2.319(10)	2.270(3)	
Mo3–O1	2.282(3)	2.314(4)	2.257(12)	2.306(3)	
Mo3–O3	2.294(2)	2.282(4)	2.305(11)	2.243(3)	
Cr–Mo1	3.317(1)	3.325(1)	3.345(1)	3.3488(4)	
Cr–Mo2	3.318(2)	3.354(1)	3.337(2)	3.3352(3)	
Cr–Mo3	3.319(2)	3.346(1)	3.336(2)	3.3031(4)	
Mo1–Mo2	3.323(2)	3.343(1)	3.407(2)	3.3085(5)	
Mo1–Mo3	3.322(2)	3.345(1)	3.297(3)	3.3279(5)	
Mo2–Mo3	3.319(1)	3.336(1)	3.314(2)	3.3510(4)	
O1–O2 ^d	2.900(3)	2.915(5)	2.955(13)	2.913	2.887–2.856
O1–O3	2.905(4)	2.928(5)	2.928(15)	2.923	2.831–2.796
O2–O3 ^d	2.904(3)	2.934(5)	2.957(14)	2.938	2.887–2.887
O1'–O2'					2.883–2.895
O1'–O3'					2.705–2.735
O2'–O3'					2.887–2.890
Angles ^d					
O1–O2–O3	60.07(8)	60.07(12)	59.39(34)	59.95	58.72–58.61
O2–O3–O1	59.90(9)	59.64(12)	60.28(34)	59.60	60.64–60.67
O3–O1–O2	60.03(8)	60.28(12)	60.33(34)	60.45	60.64–60.72
O1'–O2'–O3'					56.43–55.96
O2'–O3'–O1'					61.89–62.02
O3'–O1'–O2'					61.68–62.02
O1–Cr–O2	95.40(10)	95.32(15)	96.72(39)	94.89	92.10–91.72
O1–Cr–O3	95.47(10)	95.98(16)	96.68(46)	95.23	92.13–92.19
O2–Cr–O3	95.52(10)	96.18(15)	96.64(40)	96.43	92.10–92.31
O1'–Cr–O2'					94.64–95.34
O1'–Cr–O3'					87.72–88.13
O2'–Cr–O3'					94.64–94.82
Distance ^e <i>d</i>					
	2.038(2)	2.032(2)	1.994(6)	2.050	2.164–2.168

^a This work. ^b From ref 20. In *a* and *b*, oxygen atoms bridging both chromium and molybdenum are labeled O1–O3. ^c **WCr₆** = $[\{A-\alpha-SiO_4W_9O_{30}(OH)_3Cr_3\}_2(OH)_3]^{11-}$ from ref 35. The distances in the six CrO₆ octahedra are tabulated as O1 and O3 bridging two chromium atoms in the same Cr₃O₁₅ cluster; O2 is bridging the chromium atom and a silicon atom, O2' is bridging two chromium atoms of two different Cr₃O₁₅ clusters, and O1' and O3' are bridging both chromium and molybdenum atoms. ^d Symmetry code $-x, -y, -z$. ^e Distance between least-squares planes.

Cr–O1 and Cr–O3 (1.96 Å) ones, and also, the O1–O2 and O2–O3 distances (2.96 Å) are greater than the O1–O3 one (2.93 Å). This deformation leads to less defined ESR spectra (Figure 7).

As seen in Table 3 and Figure 7, all spectra are very complex in shape and the position of the line is not conventional. Only for the **CrDMSO** compounds, where the octahedral environment of the Cr^{III} is less rhombic-deformed, we have an almost normal representation of the powder spectra for a zero-field splitting,^{53–56} but the lines at high field do not have the normal shape. For

these spectra, we can estimate the *D* parameter at 0.2 cm⁻¹. This zero-field splitting parameter is due to the dipole–dipole interaction between two unpaired electrons or to the coupling between the electron orbital and spin angular momenta. When the rhombic deformation increases, the ESR powder spectra are less and less defined³⁵ and the *D* parameters seem to be increasing.⁵³

Conclusion

The materials described in this paper were obtained by molecular assemblies of ferrocenium radical derivatives and paramagnetic polyoxometalates. As in the previously reported materials,¹⁴ a 3-D packing of the Fe(C₅Me₅)₂⁺ units is observed with the Keggin polyanions containing paramagnetic transition

(54) Mehran, F.; Shafer, M. W.; Subba Rao, G. V. *Solid State Commun.* **1979**, *13*, 1311.

(55) MacFarlane, R. M. *J. Chem. Phys.* **1967**, *47*, 2066.

(56) MacFarlane, R. M. *Phys. Rev.* **1970**, *B1*, 989.

metal. Furthermore, a new type of structure was observed in the **FeCr(1)** compound. This structure contains perpendicular mixed stacks of $[\text{Fe}(\text{C}_5\text{Me}_5)_2^+]_3$ clusters and planar $[\text{Cr}(\text{OH})_6\text{Mo}_6\text{O}_{18}]^{3-}$, and from this point of view, it is reminiscent of that of the well-known ferromagnetic material $\text{Fe}(\text{C}_5\text{Me}_5)_2\text{-TCNE}\cdot\text{CH}_3\text{CN}$.³⁰ Unfortunately, such ferromagnetic interactions did not occur in our compound due to the absence of overlap between the spin carriers. The structural richness of this series reflects the high ability of the $\text{Fe}(\text{C}_5\text{Me}_5)_2^+$ cations to adopt different packings. Despite the very large separations between adjacent spin carriers, magnetic measurements indicate weak intermolecular antiferromagnetic interactions at low temperature. We observed that the dehydration of **FeCr(1)** by removing the 20 water molecules does not affect the magnetic properties.

The use of other polyoxometalates and other organometallic cations $[\text{M}(\text{C}_5\text{R}_5)_2^+]$: $\text{R} = \text{CH}_3, \text{H}$; $\text{M} = \text{Cr}^{\text{III}} (S = 3/2), \text{Mn}^{\text{III}} (S = 1)$ with different magnetic moments, shapes, and sizes may give rise to significant magnetic interactions. As a first result in this direction, we observed for instance, in the **FeCr(2)** compound, a shortening of Fe–Fe distances (6.741(4) Å) instead of 7.889(2) Å in **FeCr(1)**. The synthesis of the novel anhydrous salt containing the Anderson–Evans polyanion $[\text{Cr}(\text{OH})_6\text{Mo}_6\text{O}_{18}]^{3-}$ described here should enable the use of the manganese and chromium units, which are air and moisture sensitive.

Supporting Information Available: Four X-ray crystallographic files, in CIF format, are available on the Internet only. Access information is given on any current masthead page.

IC971221H